IEEE Photonics Journal
An IEEE Photonics Society Publication

Average BER of SIM-DPSK FSO System With Multiple Receivers over $\mathcal{M}$-Distributed Atmospheric Channel With Pointing Errors

Volume 9, Number 4, August 2017

Nenad D. Milosevic
Milica I. Petkovic, ***Student Member, IEEE***
Goran T. Djordjevic, ***Member, IEEE***

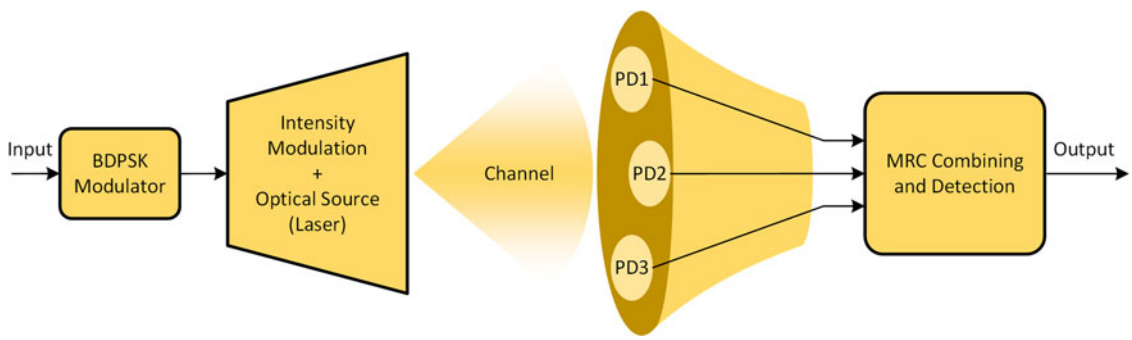

DOI: 10.1109/JPHOT.2017.2710320
1943-0655 © 2017 IEEE

Average BER of SIM-DPSK FSO System With Multiple Receivers over $\mathcal{M}$-Distributed Atmospheric Channel With Pointing Errors

Nenad D. Milosevic, Milica I. Petkovic, *Student Member, IEEE*, and Goran T. Djordjevic, *Member, IEEE*

Faculty of Electronic Engineering, University of Nis, Nis 18000, Serbia

DOI:10.1109/JPHOT.2017.2710320

Manuscript received May 8, 2017; revised May 26, 2017; accepted May 27, 2017. Date of publication June 1, 2017; date of current version July 19, 2017. This work was supported in part by Ministry of Foreign Affairs of Norway within the NORBAS project, and in part by Ministry of Education, Science and Technology Development of Republic of Serbia under Grants TR-32028 and TR-32037. Corresponding author: N. Milosevic. (e-mail: nenad.milosevic@elfak.ni.ac.rs).

Abstract: In this paper, an average bit error rate (BER) analysis of the free-space optical (FSO) system applying subcarrier intensity modulation with binary differential phase-shift keying is presented. Multiple receiver apertures are considered, when maximal-ratio combining (MRC) is employed. Intensity fluctuations due to atmospheric turbulence are modeled by Má laga ($\mathcal{M}$) distribution, taking the pointing errors effect into account. Novel closed-form average BER expression is derived in terms of Meijer's *G*-function. Utilizing derived expression, numerical results are presented and confirmed by Monte Carlo simulations. The effects of atmospheric turbulence and pointing errors parameters, as well as the number of photodetectors, on the average BER performance are discussed. Employing multiple receivers with MRC leads to the improvement of the FSO system performance. Numerical results illustrate that this improvement depends on the FSO channel conditions. In addition, it is proved that SNR unbalance scenario can seriously deteriorate system performance.

Index Terms: Atmospheric turbulence, binary differential phase-shift keying (BDPSK), bit error rate (BER), free-space optics (FSO), Má laga ($\mathcal{M}$) distribution, maximal-ratio combining (MRC), pointing errors.

1. Introduction

As a modern attractive technology, free-space optical (FSO) systems have become a solution for providing novel demands of new generation telecommunications systems. The FSO systems have a lot of benefits compared to traditional wireless radio-frequency (RF) systems. First of all, the FSO systems provide wide bandwidth and data rates close to the ones in the case of optical fiber systems. Further, the FSO technology allows a license-free transmission with easy, low-cost and simple installation [1]–[3].

The intensity fluctuations of the received optical signal are mainly caused by the atmospheric turbulence, which is a result of the refractive index random changes. Based on the experimental measurements and a number of theories for the optical signal propagation, many statistical models were established to describe the effect of atmospheric turbulence. The Gamma-Gamma distribution is adopted as a convenient one, since it provides a good matching of experimental data and theory in wide range of turbulence conditions [3]. Recently, a novel Má laga ($\mathcal{M}$) distribution is proposed as a more general model in [4]. Compared to other models, $\mathcal{M}$ distribution takes into account the effect of multiple scattered components. Hence, it can be reduced to well-known distributions, such as log-normal, K, Gamma-Gamma, Exponential, etc. [4]–[10]. Besides the atmospheric turbulence, the misalignment between FSO transmitter laser and FSO receiver photodetector is another reason for optical signal degradation. Due to many natural phenomena as strong wind, earthquakes, thermal expansion, installed FSO apertures are in motion, which results in the optical laser beam vibrations. Due to this fact, an imprecision of laser beam positioning occurs, leading to the effect called pointing errors [11]–[13]. Combined effect of the pointing errors and $\mathcal{M}$-distributed atmospheric turbulence was observed in [7]–[9].

As a well-known method to mitigate the effects of scintillation, spatial diversity techniques have been borrowed from RF networks and applied within commercial FSO systems [1], [2]. Employing selection combining (SC), equal gain combining (EGC) or maximal-ratio combining (MRC) in FSO system influenced by strong K-distributed atmospheric turbulence was observed in [14]. The FSO signal transmission over weak log-normal atmospheric turbulence channel was analyzed in [15] and [16], considering the employment of SC or switched combining (switch-and-stay and switch-and-examine combining), respectively. Implementation of the spatial diversity techniques in the FSO system considering Gamma-Gamma atmospheric turbulence, which covers conditions from weak to strong ones, was examined in [17]–[19], while the impact of the pointing errors on the same system was observed in [20], [21]. The impact of multiple scattered components, described by $\mathcal{M}$ statistical model, on the performance of the FSO system with spatial diversity techniques was analyzed in [22], [23]. Concretely, [22] examined the average bit error rate (BER) of the dual-branch FSO system applying MRC and EGC. Mutual effect of the pointing errors and $\mathcal{M}$-distributed atmospheric turbulence on the average BER performance of the MRC- and SC-based FSO system with multiple receivers was observed in [23].

Most practical FSO systems widely employ intensity fluctuation/direct detection (IM/DD) with on-off keying (OOK) scheme, primarily due to simplicity in implementation and design, as well as cost effectiveness and bandwidth efficiency. Furthermore, the interest in L-symbols pulse position modulation (L-PPM) has been raised since any decision threshold is not required unlike with the OOK scheme. Also, L-PPM is more power efficient compared to OOK, at the cost of an increased bandwidth requirement and higher system complexity. As a further solution for employed modulation within FSO system, subcarrier intensity modulation (SIM) has been borrowed from the multiple carrier RF systems, where the baseband signal is first pre-modulated with an intermediate frequency carrier, considering one of the RF modulation schemes. The RF modulator output modulates the optical source (laser) intensity. Besides providing multiple subcarrier multiplexing, the SIM technique avoids an adaptive threshold requirement as OOK, and provides lower bandwidth requirement than the PPM at the same time [1].

Inspired by works in [22], [23], which considered the FSO system with SIM and binary phase-shift keying (BPSK), we analyze the SIM FSO system employing binary differential phase-shift keying (BDPSK). The advantage of DPSK compared to PSK is in the fact that the carrier phase estimation at the receiver is not required, since the decision of the DPSK receiver is made based on the phase difference between signals received during two consecutive symbol intervals [24]. The FSO system with multiple receiver apertures is observed, when MRC is applied, since it is the optimal spatial diversity technique. Both $\mathcal{M}$-distributed atmospheric turbulence and pointing errors are taken into consideration. Novel closed-form average BER expression is derived, which is further reduced to the case when the scatter component is not taken into account (thus the Gamma-Gamma atmospheric turbulence is considered), as well as the case when the pointing error is negligible. Numerical results are presented and validated by Monte Carlo simulations.

The rest of the paper is organized as follows. The system and channel model is presented in Section 2. Section 3 gives the average BER analysis for multiple receivers FSO system. Numerical results with comments are shown in Section 2. Concluding remarks are presented in Section 5.

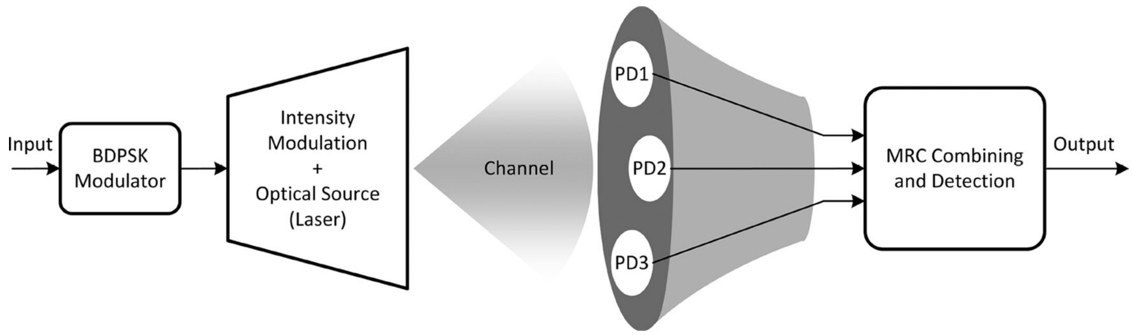

Fig. 1. System model with three photodetectors.

2. System and Channel Model

The FSO system with N photodetectors and MRC spatial diversity technique applied at the receiver is investigated. Fig. 1 shows the considered FSO system with three photodetectors. The SIM employing BDPSK is considered at the transmitter of the system, meaning that the information bits are first premodulated by electrical BDPSK modulator, whose output modulates the optical source (laser) intensity. Since SIM technique is applied, DC bias is added in order to satisfy non-negativity requirement. The laser beam is transmitted via free space, i.e., atmospheric channel. At the receiver part of the system, there are N photodetectors which collect the receiving laser beam. The independent and identically distributed (i.i.d.) channels are considered. It is assumed that the photodetectors are sufficiently spaced to provide uncorrelated scenario [14], [15]. In order to make true this assumption, the spacing between receivers should be greater than the fading correlation length. In practical scenario, this issue may be difficult to complete, due to available physical space or since the receiver spacing required for uncorrelated fading may exceed the beam diameter in power-limited links with well-collimated beams. Hence, the presented result for considered uncorrelated scenario is a lower limit case. The optical signal at the i-th receiving aperture is

$$s_i = P_t R I_i \left(1 + m s(t)\right), \ \ i = 1, \dots, N, \tag{1}$$

where P_t denotes the transmitted optical power, R is each detector responsivity, I_i represents the optical signal irradiance of the i-th channel, m is modulation index ($m = 1$), and $s(t)$ denotes the electrical signal at the BDSPK modulator output. After direct detection at the receiver, DC bias is removed and an optical-to-electrical conversion by the i-th photodetector are performed. The electrical signal of the each receiving aperture at MRC input is defined as

$$r_i = P_t R I_i s'(t) + n_i, \ \ i = 1, \dots, N, \tag{2}$$

where n_i represents the additive white Gaussian noise with zero mean and variance $\sigma_{n_i}^2$. In practice, the total field of view of all detectors needs to be covered by the laser beam footprint. For that reason, each detector area is N times smaller than the one when there is no diversity. Hence, assuming that the background radiation is the dominant source of noise, the noise variance of each aperture is N times smaller than the noise variance of the system without diversity, σ_u^2, i.e., $\sigma_{n_i}^2 = \sigma_u^2/N$ [14]. Due to different brightening of the photodetectors of different receiver branches, as well as imperfections in electronics and practical implementation, the different levels of the noise variance occur, corresponding to the unbalancing effect. Finally, the MRC spatial diversity technique and BDPSK demodulation are performed.

The received instantaneous SNR for each channel is defined as

$$\gamma_i = \frac{P_t^2 R^2 I_i^2}{2\sigma_{n_i}^2}, \ \ i = 1, \dots, N, \tag{3}$$

and the electrical SNR for i-th channel is

$$\mu_i = \frac{P_t^2 R^2}{2\sigma_{n_i}^2} \mathrm{E}^2 [I_i], \; i = 1, \ldots, N, \tag{4}$$

where $\mathrm{E}[\cdot]$ is the statistical expectation operator. When $\sigma_{n_1}^2 = ... = \sigma_{n_N}^2$, the balanced SNR scenario is considered.

The statistic of the signal intensity, I_i, is accounted for combined effect of $\mathcal{M}$-distributed atmospheric turbulence and pointing errors. As it has been already mentioned, the $\mathcal{M}$ distribution is general model, which accounts the effect of multiple scattered components. Beside the component C_L occurred due to line-of-sight (LOS) contribution, the component C_{CS} scattered by the eddies on the propagation axis is also included (the same as in the Gamma-Gamma distribution). The component C_{CS} is coupled to the component C_L. Furthermore, the $\mathcal{M}$ distribution also includes the component scattered to the receiver by the off-axis eddies, denoted by C_{GS}, which is statistically independent from both C_L and C_{CS} [4]–[9]. It is assumed that the pointing errors effect is also taken into consideration, thus the probability density function (PDF) of I_i is expressed as [7, (21)]

$$f_{I_i}(I_i) = \frac{\xi^2 \mathrm{A}}{2} I_i^{-1} \sum_{k=1}^{\beta} a_k \left(\frac{\alpha\beta}{g\beta + \Omega'}\right)^{-\frac{\alpha+k}{2}} G_{1,3}^{3,0}\left(\frac{\alpha\beta I_i}{(g\beta+\Omega')A_0} \middle| \begin{matrix} \xi^2+1 \\ \xi^2, \alpha, k \end{matrix} \right), \tag{5}$$

where $G_{p,q}^{m,n}(\cdot)$ is Meijer's G-function [25, (9.301)], and constants A and a_k are defined as [7, (8)]

$$\mathrm{A} \triangleq \frac{2\alpha^{\frac{\alpha}{2}}}{g^{1+\frac{\alpha}{2}}\Gamma(\alpha)} \left(\frac{g\beta}{g\beta+\Omega'}\right)^{\beta+\frac{\alpha}{2}}, \; a_k \triangleq \binom{\beta-1}{k-1} \frac{(g\beta+\Omega')^{1-\frac{k}{2}}}{(k-1)!} \left(\frac{\Omega'}{g}\right)^{k-1} \left(\frac{\alpha}{\beta}\right)^{\frac{k}{2}}, \tag{6}$$

with natural number β representing the amount of fading parameter, and a positive parameter α related to the effective number of large-scale cells of the scattering process. The parameter g denotes the average power of the scattering component received by off-axis eddies, which is defined as $g = \mathrm{E}\left[|C_{GS}|^2\right] = 2b_0(1-\rho_M)$, where $2b_0$ is the average power of the total scatter components determined as $2b_0 = \mathrm{E}\left[|C_{CS}|^2 + |C_{GS}|^2\right]$, and the parameter ρ_M $(0 \le \rho_M \le 1)$ defines the amount of scattering power coupled to the LOS component. Furthermore, the average power from the coherent contributions is $\Omega' = \Omega + 2b_0\rho_M + 2\sqrt{2b_0\rho_M\Omega}\cos(\phi_A - \phi_B)$, where $\Omega = \mathrm{E}\left[|C_L|^2\right]$ is the average power of the LOS, and ϕ_A and ϕ_B are deterministic phases of the LOS and the coupled to LOS scatter terms, respectively [4].

The parameter ξ is defined as the ratio between equivalent beam radius at the receiver, a_e, and jitter standard deviation, σ_s, i.e., $\xi = a_e/(2\sigma_s)$. Further, a_e is related to the optical beam radius at the distance d, a_d, as $a_e^2 = a_d^2 \sqrt{\pi}\mathrm{erf}(v)/\left(2v\exp\left(-v^2\right)\right)$, with $A_0 = \mathrm{erf}^2(v)$, $v = \sqrt{\pi}a/\left(\sqrt{2}a_d\right)$, and a is the radius of each circular detector [12], [13].

After some mathematical manipulations, using the instantaneous SNR definition in (3) and the PDF in (5), the PDF of γ_i is derived as

$$f_{\gamma_i}(\gamma_i) = \frac{\xi^2 \mathrm{A}}{4\gamma_i} \sum_{k=1}^{\beta} a_k \left(\frac{\alpha\beta}{g\beta+\Omega'}\right)^{-\frac{\alpha+k}{2}} G_{1,3}^{3,0}\left(\frac{\alpha\beta\kappa(g+\Omega')}{g\beta+\Omega'} \sqrt{\frac{\gamma_i}{\mu_i}} \middle| \begin{matrix} \xi^{2+1} \\ \xi^2, \alpha, k \end{matrix} \right), \tag{7}$$

where $\kappa = \xi^2/\left(\xi^2+1\right)$. The electrical SNR is determined based on (4) and (5) as

$$\mu_i = \frac{P_t^2 R^2}{2\sigma_n^2} {A_0}^2 \kappa^2 \left(g+\Omega'\right)^2, \; i = 1, \ldots, N. \tag{8}$$

Note that it holds $\mu_i = \mu/N$, where μ is electrical SNR when no diversity is applied [15].

3. Average BER Analysis

In this Section, the average BER analysis of SIM-BDPSK based FSO system with multiple receivers and MRC is presented. Using well-known expression for the BDPSK system [24], the average BER can be found as

$$P_b = \frac{1}{2} \int_{\Gamma} f_{\Gamma}(\Gamma) \exp\left(-\sum_{i=1}^{N} \gamma_i\right) d\Gamma, \tag{9}$$

where $f_{\Gamma}(\Gamma) = f_{\gamma_1,\ldots,\gamma_N}(\gamma_1, \cdots, \gamma_N)$ is the joint PDF of N instantaneous SNRs at the input of the MRC. Using standard mathematical manipulations, average BER in (9) is re-written as

$$\begin{aligned} P_b &= \frac{1}{2} \int_{\Gamma} f_{\Gamma}(\Gamma) \prod_{i=1}^{N} \exp(-\gamma_i) d\Gamma = \frac{1}{2} \prod_{i=1}^{N} \int_0^{\infty} f_{\gamma_i}(\gamma_i) \exp(-\gamma_i)\, d\gamma_i \\ &= \frac{1}{2} \prod_{i=1}^{N} \sum_{k=1}^{\beta} \frac{\xi^2 A a_k}{4} \left(\frac{\alpha\beta}{g\beta + \Omega'}\right)^{-\frac{\alpha+k}{2}} \int_0^{\infty} \gamma_i^{-1} \exp(-\gamma_i) \quad G_{1,3}^{3,0}\left(\frac{\alpha\beta\kappa(g+\Omega')}{g\beta+\Omega'} \sqrt{\frac{\gamma_i}{\mu_i}} \,\middle|\, \begin{matrix} \xi^2+1 \\ \xi^2,\ \alpha,\ k \end{matrix}\right) d\gamma_i. \end{aligned} \tag{10}$$

After representing the exponential function is terms of the Meijer's G-function by [26, (01.03.26.0004.01)] as $\exp(-\gamma_i) = G_{0,1}^{1,0}(\gamma_i|_0^-)$, integral in (10) is solved by utilizing [26, (07.34.21.0013.01)] as

$$\begin{aligned} P_b = \frac{1}{2} \prod_{i=}^{N} \sum_{k=1}^{\beta} \frac{\xi^2 A a_k 2^{\alpha+k-4}}{\pi} \left(\frac{\alpha\beta}{g\beta+\Omega'}\right)^{-\frac{\alpha+k}{2}} \\ \times G_{3,6}^{6,1}\left(\frac{\alpha^2\beta^2\kappa^2(g+\Omega')^2}{16\mu_i(g\beta+\Omega')^2} \,\middle|\, \begin{matrix} 1,\ \frac{1+\xi^2}{2},\ \frac{2+\xi^2}{2} \\ \frac{\xi^2}{2},\ \frac{1+\xi^2}{2},\ \frac{\alpha}{2},\ \frac{1+\alpha}{2},\ \frac{k}{2},\ \frac{1+k}{2} \end{matrix}\right). \end{aligned} \tag{11}$$

After permutation of the parameters in the Meijer's G-function by [26, (07.34.04.0003.01) and (07.34.04.0004.01)], the order of Meijer's G-function in (11) is reduced based on [26, (07.34.03.0002.01)]. The final form of the derived average BER expression is

$$P_b = \frac{1}{2} \prod_{i=1}^{N} \sum_{k=1}^{\beta} \frac{\xi^2 A a_k 2^{\alpha+k-4}}{\pi} \left(\frac{\alpha\beta}{g\beta+\Omega'}\right)^{-\frac{\alpha+k}{2}} G_{2,5}^{5,1}\left(\frac{\alpha^2\beta^2\kappa^2(g+\Omega')^2}{16\mu_i(g\beta+\Omega')^2} \,\middle|\, \begin{matrix} 1,\ \frac{2+\xi^2}{2} \\ \frac{\xi^2}{2},\ \frac{\alpha}{2},\ \frac{1+\alpha}{2},\ \frac{k}{2},\ \frac{1+k}{2} \end{matrix}\right). \tag{12}$$

If $\rho_M = 1$, the average power of scattering component received by off-axis eddies is $g = 0$ and the average power from the coherent contributions is $\Omega' = 1$. In that case, the $\mathcal{M}$ distribution is reduced to the Gamma-Gamma distribution. Then, the product $A \times a_k$ is nonzero only when $k = \beta$, and it holds $A \times a_k = 2\alpha^{\frac{\alpha+\beta}{2}} \beta^{\frac{\alpha+\beta}{2}} / (\Gamma(\alpha)\Gamma(\beta))$, and the BER in (12) is reduced to

$$P_b^{GG} = \frac{1}{2} \prod_{i=1}^{N} \frac{\xi^2 2^{\alpha+\beta-3}}{\pi\Gamma(\alpha)\Gamma(\beta)} \left(\frac{1}{g\beta+\Omega'}\right)^{-\frac{\alpha+\beta}{2}} G_{2,5}^{5,1}\left(\frac{\alpha^2\beta^2\kappa^2(g+\Omega')^2}{16\mu_i(g\beta+\Omega')^2} \,\middle|\, \begin{matrix} 1,\ \frac{2+\xi^2}{2} \\ \frac{\xi^2}{2},\ \frac{\alpha}{2},\ \frac{1+\alpha}{2},\ \frac{\beta}{2},\ \frac{1+\beta}{2} \end{matrix}\right). \tag{13}$$

When the pointing errors effect is very small and can be neglected, then the parameter $\xi \to \infty$. The intensity fluctuations of the received optical signal are assumed to originate only from the $\mathcal{M}$-distributed atmospheric turbulence. By taking the limit of (12) for $\xi \to \infty$, after applying [26, (07.34.25.0007.01), (07.34.25.0006.01) and (06.05.16.0002.01)], the average BER for the

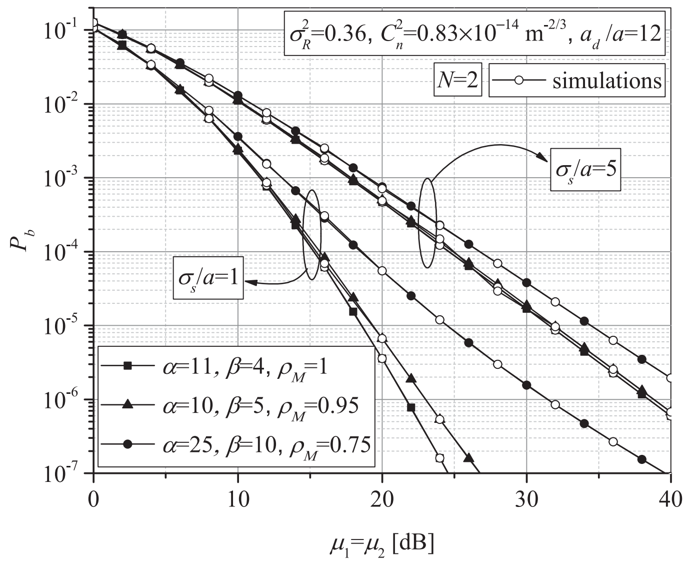

Fig. 2. Average BER of dual-branch FSO system for different values of ρ_M and various pointing errors strengths.

non-pointing errors FSO system is derived as

$$P_b^{\xi\to\infty} = \frac{1}{2}\prod_{i=1}^{N}\sum_{k=1}^{\beta}\frac{\mathrm{A}a_k 2^{\alpha+k-3}}{\pi}\left(\frac{\alpha\beta}{g\beta+\Omega'}\right)^{-\frac{\alpha+k}{2}} G_{1,4}^{4,1}\left(\frac{\alpha^2\beta^2(g+\Omega')^2}{16\mu_i(g\beta+\Omega')^2}\middle|\begin{matrix}1\\ \frac{\alpha}{2},\ \frac{1+\alpha}{2},\ \frac{k}{2},\ \frac{1+k}{2}\end{matrix}\right). \quad (14)$$

4. Numerical and Simulations Results

In this Section, numerical results are presented together with Monte Carlo simulations to confirm analytical results. The intensity of atmospheric turbulence is determined by the Rytov variance defined as $\sigma_R^2 = 1.23C_n^2\left(\frac{2\pi}{\lambda}\right)^{7/6} d^{11/6}$, with the wavelength λ, the FSO link distance d, and the refractive index structure parameter C_n^2. Numerical results are obtained based on the channel parameters given in [4]–[7], which represent some experimental measurements. Jitter standard deviation, σ_s, is used to describe the strength of pointing errors. The radius of a circular detector aperture takes a value $a = 5$ cm, wavelength employed in FSO link is $\lambda = 785$ nm and the FSO link distance is $d = 1$ km. Normalized average optical power of the FSO hop is assumed $\Omega + 2b_0 = 1$.

Fig. 2 shows the average BER dependence on the electrical SNR of the dual-branch FSO system, considering different values of the pointing errors strength, $\sigma_s/a = 1$ and $\sigma_s/a = 5$. The atmospheric turbulence strength is defined by results from [7], which are obtained by experiments performed in University of Waseda, Japan, on the 15th October, 2009. For given parameters the Rytov variance is the same, thus the scattering component has decisive impact on the average BER performance. Higher values of the parameter ρ_M leads to the better system performance. When $\rho_M = 1$, the performance is the best (and the amount of the power scattered to the receiver by the off-axis eddies, i.e., power of C_{GS}, is equal to zero), so the FSO system is affected by Gamma-Gamma atmospheric turbulence. The component C_{GS} has stronger impact on the average BER when the pointing error is weak.

Fig. 3 is obtained by utilizing the values of the parameters given in [6, Table 1], and presents the average BER versus jitter standard deviation for different atmospheric turbulence conditions. Better system performance is achieved when atmospheric turbulence is weak (σ_R^2 is lower), as well when the pointing error is poor (σ_s is lower). In addition, the impact of atmospheric turbulence

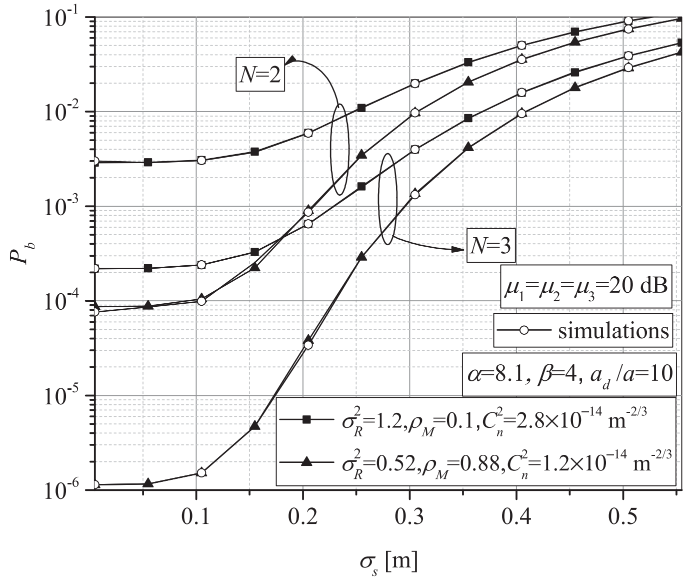

Fig. 3. Average BER of FSO system for different pointing errors strength in various atmospheric turbulence conditions.

on average BER is greater when the pointing error is weak. The improvement of the system performance with the implementation of the greater number of photodetectors can also be observed from Fig. 3. The SNR gain obtained by employing multiple receivers is dependent on pointing errors conditions. For example, for $\sigma_R^2 = 0.52$, by increasing the number of photodetectors from $N = 2$ to $N = 3$, the average BER is reduced about 69.44 and 3.87 times when $\sigma_s = 0.1$ m and $\sigma_s = 0.4$ m, respectively. Further, the SNR gain is also dependent on atmospheric turbulence. For example, for $\sigma_s = 0.1$ m, by increasing the number of photodetectors from $N = 2$ to $N = 3$, the average BER is reduced about 72 and 13 times, when $\sigma_R^2 = 0.52$ and $\sigma_R^2 = 1.2$, respectively. To conclude, the performance improvement due to increased number of photodetectors is dependent on the FSO channel conditions.

The average BER versus electrical SNR for different number of photodetectors and different amount of scattering power coupled to the LOS (or the average power of the scattering component received by off-axis eddies) is depicted in Fig. 4. Implementation of greater number of photodetectors at the receiver leads to the system performance improvement and significant SNR gain. For example, in order to achieve $P_b = 10^{-5}$ when $\rho_M = 0.95$, electrical SNR gain is about 20 dB and 6 dB by increasing of the number of photodetectors from $N = 1$ to 2 and $N = 2$ to 3, respectively. With parameter ρ_M decreasing, corresponding gains increases.

In Fig. 5, the average BER dependence on electrical SNR is presented, considering the signals power on the photodetectors are not equal, i.e., unbalanced SNR scenario ($\mu_1 \neq \mu_2$). The system performance could be considerably degraded due to SNR unbalancing. This kind of degradation is dependent on the atmospheric turbulence conditions. For example, for given average BER of 2.95×10^{-4}, the required electrical SNR μ_1 for the case of balanced SNRs ($\mu_2 = \mu_1$) is about 10 dB smaller compared to the case of unbalanced SNRs ($\mu_2 = \mu_1/2$) for strong atmospheric turbulence ($\sigma_R^2 = 1.2$). When optical signal transmission is affected by weak atmospheric turbulence ($\sigma_R^2 = 0.52$), the electrical SNR μ_1 penalty of about 6 dB is paid due to the same SNR unbalancing.

We pay our attention on scintillation reduction by applying diversity technique. This negative effect can be also reduced by increasing the area of a photodetector, which enables integration of various intensities incident on particular parts of the lens. This technique is known as aperture averaging and is described in details in [3]. By applying similar approach as in [27], the aperture averaging effect could be considered in our scenario that will be the topic of our further work.

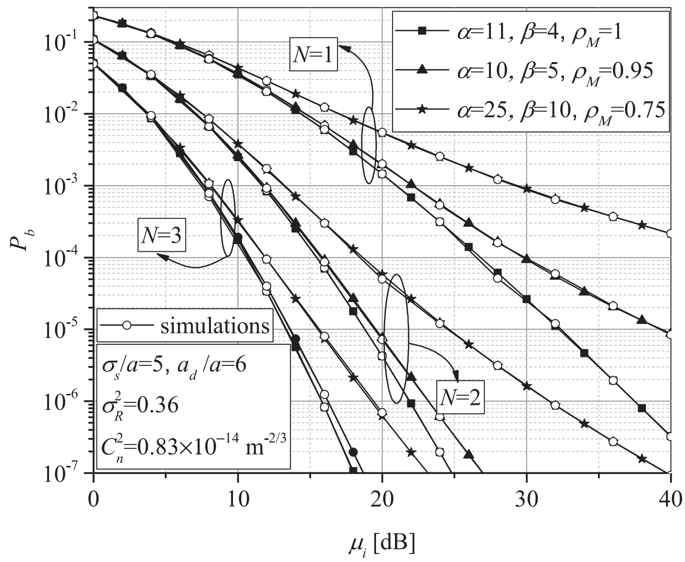

Fig. 4. Average BER in the function of μ_i for different number of photodetectors.

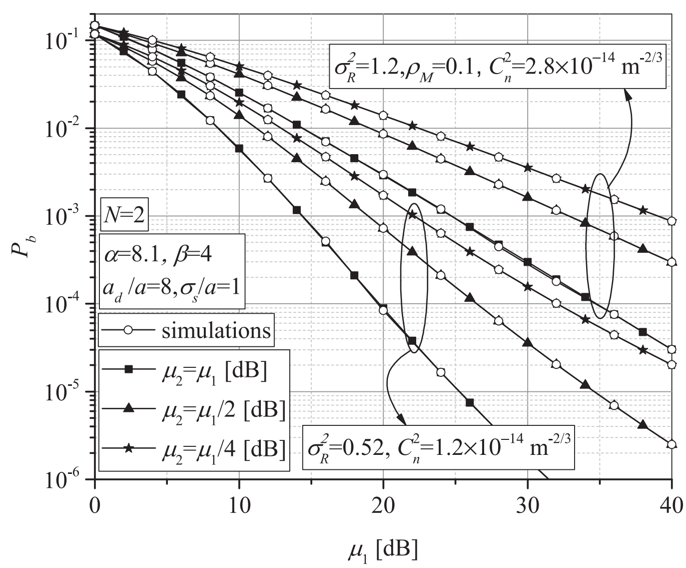

Fig. 5. Average BER in the function of the electrical SNR for unbalanced SNR scenario.

5. Conclusion

This paper has analyzed the average BER of multiple receivers SIM-DPSK FSO system employing MRC as the optimal diversity technique. Intensity fluctuations due to atmospheric turbulence are modeled by general $\mathcal{M}$ distribution considering the pointing errors effect. Novel closed-form average BER expression has been derived, which has been further reduced to some simpler cases. Derived expressions have been utilized to obtain numerical results, which have been validated by Monte Carlo simulations. The effect of different system and channel parameters on the average BER performance has been examined and commented.

It has been concluded that the component scattered to the receiver by the off-axis eddies (which represents the generality of $\mathcal{M}$ distribution) has an important impact on the average BER performance, particularly when the positioning of the FSO aperture is good and the pointing error is weak. Furthermore, employing of multiple photodetectors in FSO system results in significant performance improvement, especially under good FSO channel conditions (weak atmospheric turbulence and poor pointing errors). In addition, the SNR unbalance scenario has been observed, which proves to be an important issue during FSO system design and implementation, since it can degrade system performance, especially in weak atmospheric turbulence conditions.

Since the atmospheric turbulence results in slowly-varying fading, remaining constant over a large number of transmitted bits, the outage probability is also a relevant metric of signal transmission quality. Determination of the outage probability for the system described here is in the scope of our further investigations.

Acknowledgement

The authors wish to thank the anonymous reviewers and Associate Editor for their valuable time and comments that improved the quality of our manuscript.

References

[1] Z. Ghassemlooy, W. Popoola, and S. Rajbhandari, *Optical Wireless Communications: System and Channel Modelling with MATLAB*. Boca Raton, FL, USA: CRC Press, 2013.
[2] M. A. Khalighi and M. Uysal, “Survey on free space optical communication: A communication theory perspective,” *IEEE Commun. Surveys Tuts.*, vol. 16, no. 4, pp. 2231–2258, Oct.–Dec. 2014.
[3] L. C. Andrews and R. N. Philips, *Laser Beam Propagation through Random Media*. 2nd ed. Washington, DC, USA: Spie Press, 2005.
[4] A. Jurado-Navas, J. M. Garrido-Balsells, J. F. Paris, and A. Puerta-Notario, “A unifying statistical model for atmospheric optical scintillation,” in, *Numerical Simulations of Physical and Engineering Processes*. Rijeka, Croatia: Intech, 2011.
[5] A. Jurado-Navas, J. M. Garrido-Balsells, J. F. Paris, M. Castillo-Vzquez, and A. Puerta-Notario, “General analytical expressions for the bit error rate of atmospheric optical communication systems,” *Opt. Lett.*, vol. 36, no. 20, pp. 4095–4097, Oct. 2011.
[6] H. Samimi and M. Uysal, “Performance of coherent differential phase-shift keying free-space optical communication systems in M-distributed turbulence,” *IEEE/OSA J. Opt. Commun. Netw.* vol. 5, no. 7, pp. 704–710, Jul. 2013.
[7] A. Jurado-Navas, J. M. Garrido-Balsells, J. F. Paris, M. Castillo-Vzquez, and A. Puerta-Notario, “Impact of pointing errors on the performance of generalized atmospheric optical channels,” *Opt. Exp.*, vol. 20, no. 11, pp. 12550–12562, 2012.
[8] I. S. Ansari, H. AlQuwaiee, E. Zedini, and M.–S. Alouini, “Information theoretical limits of free-space optical links,” in *Optical Wireless Communications—An Emerging Technology*, New York, NY, USA: Springer-Verlag, 2016.
[9] H. Samimi and M. Uysal, “End-to-end performance of mixed RF/FSO transmission systems,” *IEEE/OSA J. Opt. Commun. Netw.*, vol. 5, no. 11, pp. 1139–1144, Nov. 2013.
[10] G. T. Djordjevic, M. I. Petkovic, A. M. Cvetkovic, and G. K. Karagiannidis, “Mixed RF/FSO relaying with outdated channel state information,” *IEEE J. Sel. Areas Commun.*, vol. 33, no. 9, pp. 1935–1948, Sep. 2015.
[11] S. Arnon, “Effects of atmospheric turbulence and building sway on optical wireless-communication systems,” *Opt. Lett.*, vol. 28, no. 2, pp. 129–131, Jan. 2003.
[12] A. A. Farid and S. Hranilovic, “Outage capacity optimization for free space optical links with pointing errors,” *J. Lightw. Technol.*, vol. 25, no. 7, pp. 1702–1710, Jul. 2007.
[13] H. G. Sandalidis, T. A. Tsiftsis, and G. K. Karagiannidis, “Optical wireless communications with heterodyne detection over turbulence channels with pointing errors,” *J. Lightw. Technol.*, vol. 27, no. 20, pp. 4440–4445, Oct. 2009.
[14] T. A. Tsiftsis, H. G. Sandalidis, G. K. Karagiannidis, and M. Uysal, “Optical wireless links with spatial diversity over strong atmospheric turbulence channels,” *IEEE Trans. Wireless Commun.*, vol. 8, no. 2, pp. 951–957, Feb. 2009.
[15] W. O. Popoola, Z. Ghassemlooy, J. I. H. Allen, E. Leitgeb, and S. Gao, “Free-space optical communication employing subcarrier modulation and spatial diversity in atmospheric turbulence channel,” *IET Optoelectron.*, vol. 2, no. 1, pp. 16–23, Feb. 2008.
[16] H. Moradi, H. H. Refai, and P. G. LoPresti, “Switch-and-stay and switch-and-examine dual diversity for high-speed free-space optics links,” *IET Optoelectron.*, vol. 6, no. 1, pp. 34–42, Feb. 2012.
[17] W. Zixiong, W. Zhong, S. Fu, C. Lin, “Performance comparison of different modulation formats over free-space optical (FSO) turbulence links with space diversity reception technique,” *IEEE Photon. J.*, vol. 1, no. 6, pp. 277–285, Dec. 2009.
[18] M. I. Petkovic and G. T. Djordjevic, “Outage performance of SSC receiver in FSO system with Gamma-Gamma atmospheric turbulence,” in *Proc. 12th Int. SAUM Conf. Syst., Autom. Control Meas.*, Nis, Serbia, Nov. 2014, pp. 324–327.
[19] G. T. Djordjevic, M. I. Petkovic, J. A. Anastasov, P. N. Ivanis, and Z. M. Marjanovic, “On the effects of correlation on outage performance of FSO unbalanced multibranch SC receiver,” *IEEE Photon. Technol. Lett.*, Nis, Serbia, vol. 28, no. 12, pp. 1348–1351, Jun. 2016.
[20] M. R. Bhatnagar and Z. Ghassemlooy, “Performance evaluation of FSO MIMO links in Gamma-Gamma fading with pointing errors,” in *Proc.IEEE Int. Conf. Commun.*, London, U.K., 2015, pp. 5084–5090.

[21] M. R. Bhatnagar and Z. Ghassemlooy, “Performance analysis of Gamma-Gamma fading FSO MIMO links with pointing errors,” *J. Lightw. Technol.*, vol. 34, no. 9, pp. 2158–2169, May 2016.
[22] R. Wang, P. Wang, T. Cao, L. Guo, and Y. Yan, “Average bit error rate performance analysis of subcarrier intensity modulated MRC and EGC FSO systems with dual branches over M distribution turbulence channels,” *Optoelectron. Lett.*, vol. 11, no. 49, pp. 281–285, Jul. 2015.
[23] L. Yang, M. O. Hasna, and X. Gao, “Asymptotic BER analysis of FSO with multiple receive apertures over -distributed turbulence channels with pointing errors,” *Opt. Exp.*, vol. 2, no. 15, pp. 18238–18245, 2014.
[24] J. G. Proakis, *Digital Communications*. 4th ed. New York, NY, USA: McGraw-Hill, 2001.
[25] I. Gradshteyn and I. Ryzhik, *Table of Integrals, Series, and Products*, 5th ed. New York, NY, USA: Academic, 1994.
[26] The Wolfarm Functions Site, 2008. [Online] Available: http:/functions.wolfarm.com
[27] M.-A. Khalighi, N. Schwartz, N. Aitamer, and S. Bourennane, “Fading reduction by aperture averaging and spatial diversity in optical wireless systems,” *J. Opt. Commun. Netw.*, vol. 1, pp. 580–593, 2009.